EUSIPCO 2013 1569742569

SIMULATION METHODOLOGY FOR HYBRID FILTER BANK ANALOG TO DIGITAL CONVERTERS

Boguslaw Szlachetko[*,**], *Olivier Venard*[*,***]

[*]Dpt of Systems Engineering, ESIEE Paris, Noisy Le Grand, France
[**]Dpt of Electronics,Wroclaw University of Technology, Wroclaw, Poland
[***]LaMIPS, Laboratoire commun NXP-CRISMAT, Caen, France

ABSTRACT

The paper studies the problem of designing and simulating the high speed wide-band Analog-to-Digital Converters (ADC) working in bandpass scenario. Such ADCs play a crucial role in Software Defined Radio (SDR) technology or Cognitive Radio (CR). One approach to circumvent present-days limits of ADC technologies is to split the analog input signal into multiple components and then sample them with ADCs in parallel. In this paper the frequency splitting approach is implemented using Hybrid Filter Bank ADC (HFB ADC). The proper simulation methodology of the HFB ADC remains a challenge. Special care should be taken for utilizing real valued signal and filter coefficients at every step of calculation. When computation are done in the frequency domain, the nulls in the spectrum may give rise to singularities. A shifted Fourier Transform is proposed to get rid of this.

Index Terms— shifted Fourier transform, hybrid filter bank, bandpass sampling, parallel ADC, simulation methodology

1. INTRODUCTION

The HFB ADC architecture belong to the well known class of multirate system [1]. There exist many practical implementations of multirate system in communication, speech processing, image compression and voice privacy system. During the last decades, the ADC architectures based on parallel sampling [2] have received a strong interest, as parallel architectures (both Time Interleaved [3] and Filter Bank based [4]) are seen as being able to overcome the technological bottleneck of wide band sampling with high resolution. Both parallel architecture suffer from sensitivity to imperfections and require calibration to reach state of the art performances [5, 6, 7]. Digitally assisted architecture for the purpose of calibration offer promising perspectives as the relative energy cost of digital electronic compared to the analog one used in ADC have decreased roughly speaking ten time faster over the past years [8]. Therefore HFB ADC architecture is one of the natural candidate to design a high-speed, wide-band, high resolution ADC for CR/SDR systems.

HFB ADC relies on sub-band sampling [2] and is derived from Perfect Reconstruction (PR) digital Filter Bank (FB) [1]. The HFB ADC (Fig. 1) splits input signal into M sub-bands using analog filter bank, producing M-channel analog signals. Signals in each channel are sampled by a sub-channel ADC, then up-sampled and finally discrete time synthesis filter bank is used to reconstruct the digital signal. Nyquist theory states that sampling frequency should be two times the bandwidth, thus the ADCs sampling frequency can be M times lower, because they deal with sub-band signals.

Existing approaches to HFB always make the assumption that the input signal is strictly limited to the band of interest [6, 9]. Thus the sampled signal may only suffer from in-band aliasing distortion. This is indeed a strong assumption which may appear quite optimistic in view of scenario where wireless channel dedicated to a cognitive communication may be crowded. This remains true even if we consider the shape of the receiver band-pass filter. It is thus important to understand the impact of the aliasing caused by the "out of band" energy on the performance of the HFB ADCs. Designing and simulating wide-band, high speed band-pass ADC for use in CR/SDR systems is quite specific and special care should be taken for the system simulation. Usually multirate systems utilize only digital signals, while in our case the input is an analog signal with very wide spectrum. Therefore the analog signals have to be sampled in the multirate structure, which raises the problem of the aliasing for the unwanted signals, but also for the wanted signals, i.e. bandpass sampling. In addition, system simulation of HFB ADCs have also to model properly the analog filters in the digital domain.

2. HYBRID FILTER BANK AD CONVERTER FOR SAMPLING BANDPASS RF SIGNALS

Let us consider a signal, $X(j\Omega)$, having a spectrum of interest limited to:

$$B = (-\Omega_2, -\Omega_1) \cup (\Omega_1, \Omega_2), \tag{1}$$

The research leading to these results has received funding from the European Seventh Framework Program under grant agreement n° 230688.

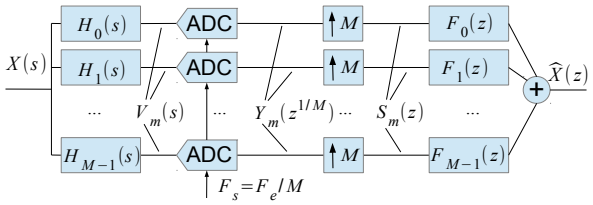

Fig. 1. The hybrid filter bank architecture of ADC

$$X(j\Omega) = 0 \text{ for } \Omega \notin B, \tag{2}$$

with Ω being the continuous angular frequency from $-\infty$ to ∞ in [πrad/s]. Such signal can be sampled using a sampling frequency $\Omega_e \geq 2(\Omega_2 - \Omega_1)$.

Let $H_m(j\Omega)$ be the transfer function of the *m*-th filter from the Analysis Filter Bank (AFB) - Figure 1. Then the output of this channel is

$$V_m(j\Omega) = X(j\Omega)H_m(j\Omega). \tag{3}$$

The AFB splits the band of interest, B, into M uniform sub-bands. Each sub-bands is then sampled using sampling frequency M times lower than desired frequency $1/T_e$. The spectrum at the output of each ADC is given by

$$Y_m(e^{j\frac{\omega}{M}}) = \frac{1}{MT_e}\sum_{l=-\infty}^{\infty} V_m\left(j\left(\frac{\omega}{MT_e} - \frac{2\pi l}{MT_e}\right)\right), \tag{4}$$

with $\Omega = \dfrac{\omega}{MT_e}$.

Because of (2) the above sum has nonzero element only for $l = 1, \ldots, M-1$, hence we obtain

$$Y_m(e^{j\frac{\omega}{M}}) = \frac{1}{MT_e}\sum_{l=0}^{M} V_m\left(j\left(\frac{\omega}{MT_e} - \frac{2\pi l}{MT_e}\right)\right). \tag{5}$$

Consequently the up-sampled signal is given by

$$S_m(e^{j\omega}) = \frac{1}{MT_e}\sum_{l=0}^{M} V_m\left(j\left(\frac{\omega}{T_e} - \frac{2\pi l}{MT_e}\right)\right). \tag{6}$$

Without loss of generality, let $\Omega_2 - \Omega_1 = 1$ [πrad/s] hence the normalized sampling frequency is $1/T_e = 1$. Using the notation

$$\omega_M^{(l)} = \left(\frac{\omega}{T_e} - \frac{2\pi l}{MT_e}\right) = \left(\omega - \frac{2\pi l}{M}\right), \tag{7}$$

we obtain

$$S_m(e^{j\omega}) = \frac{1}{M}\sum_{l=0}^{M} V_m\left(j\omega_M^{(l)}\right). \tag{8}$$

Combining (3) and (8) the HFB ADC output signal is given by

$$\widehat{X}(e^{j\omega}) = \frac{1}{M}\sum_{l=0}^{M} X\left(j\omega_M^{(l)}\right)\sum_{m=0}^{M-1} F_m(e^{j\omega})H_m\left(j\omega_M^{(l)}\right). \tag{9}$$

The classical form of this equation is

$$\widehat{X}(e^{j\omega}) = X(j\omega)T_0(e^{j\omega}) + \sum_{l=1}^{M-1} X\left(j\omega_M^{(l)}\right)T_l(e^{j\omega}), \tag{10}$$

where $T_0(e^{j\omega})$ is the system distortion function:

$$T_0(e^{j\omega}) = \frac{1}{M}\sum_{m=0}^{M-1} F_m(e^{j\omega})H_m(j\omega), \tag{11}$$

$\sum_{l=1}^{M} T_l(e^{j\omega})$ is the system aliasing function

$$T_l(e^{j\omega}) = \frac{1}{M}\sum_{m=0}^{M-1} F_m(e^{j\omega})H_m\left(j\omega_M^{(l)}\right). \tag{12}$$

The HFB system defined by (10) has the PR property if

$$T_0(e^{j\omega}) = e^{j\omega d} \text{ and } T_l(e^{j\omega}) = 0 \text{ for } l \neq 0. \tag{13}$$

This means that the system distortion function have to be a pure delay and all the aliasing terms have to be equal to zero. Equivalently, these conditions can be rewritten in a matrix form as follows

$$\frac{1}{M}\mathbf{H}(j\omega)\mathbf{F}(e^{j\omega}) = \mathbf{T}(e^{j\omega}), \tag{14}$$

where $\mathbf{F}(e^{j\omega}) = [F_0(e^{j\omega}), \ldots, F_{M-1}(e^{j\omega})]^T$ is the vector of frequency response for the synthesis filter bank, $\mathbf{H}(j\omega)$ is the matrix of modulated frequency response of the AFB

$$\begin{bmatrix} H_0(j\omega) & \ldots & H_{M-1}(j\omega) \\ \vdots & H_m(j\omega_M^{(l)}) & \vdots \\ H_0(j\omega_M^{(M-1)}) & \ldots & H_{M-1}(j\omega_M^{(M-1)}) \end{bmatrix} \tag{15}$$

and $\mathbf{T}(e^{j\omega})$ is the vector of frequency response for the distortion and aliasing transfer functions

$$[T_0(e^{j\omega}), \ldots, T_{M-1}(e^{j\omega})]^T = [e^{j\omega d}, 0, \ldots, 0]^T. \tag{16}$$

Thus the frequency response of the synthesis filter bank can be calculated by solving (14) for $\mathbf{F}(e^{j\omega})$.

2.1. Equivalent-Digital Filter Bank

If the input signal does not fulfill strictly the bandpass assumption (2), we should take into account all the aliasing terms in (4):

$$Y_m(e^{j\frac{\omega}{M}}) = \frac{1}{M}\sum_{l=-\infty}^{\infty} V_m\left(j\left(\frac{\omega}{M} - \frac{2\pi l}{M}\right)\right), \tag{17}$$

hence

$$\widehat{X}(e^{j\omega}) = X(j\omega)T_0(e^{j\omega}) + \sum_{\substack{l=-\infty \\ l\neq 0}}^{\infty} X\left(j\omega_M^{(l)}\right)T_l(e^{j\omega}). \tag{18}$$

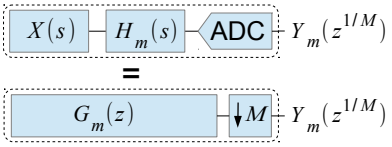

Fig. 2. The equivalent-digital analysis filter bank

In this case the system distortion function remains the same as in (10) but now there are an infinite number of aliasing terms and thus an infinite number of linear equations.

To handle this case we introduce the equivalent-digital analysis filter bank $\mathbf{G}(e^{j\omega})$. Instead of using continuous domain transfer function, the equivalent-digital system (presented in Figure 2) is used in our design. Hence the assumed input signal $X(j\Omega)$ is multiplied by the transfer functions of the input filters, then the product is sampled at the angular sampling frequency Ω_e and we obtain the equivalent-digital filter bank modulation matrix $\mathbf{G}(e^{j\omega})$ defined as

$$\begin{bmatrix} G_0(e^{j\omega}) & \dots & G_{M-1}(e^{j\omega}) \\ \vdots & G_m(e^{j\omega}W_M^l) & \vdots \\ G_0(e^{j\omega}W_M^{M-1}) & \dots & G_{M-1}(e^{j\omega}W_M^{M-1}) \end{bmatrix},$$

where $W_M^l = e^{-j2\pi l/M}$, as for digital FB [1].

It should be noted that the equivalent-digital transfer functions $G_m(e^{j\omega})$ does not depend only on the analog analysis filters but also on the "out of band" input signal. All the "out of band" signal is first filtered in the continuous domain and then aliased to the frequency interval $\omega \in [-\pi, \pi]$ through the sampling process.

The formula (14) can be rewritten using the equivalent-digital AFB to calculate the synthesis FB $\mathbf{F}(e^{j\omega})$ from $\mathbf{G}(e^{j\omega})$:

$$\frac{1}{M}\mathbf{G}(e^{j\omega})\mathbf{F}(e^{j\omega}) = \mathbf{T}(e^{j\omega}). \tag{19}$$

It is worth noting that the matrix $\mathbf{H}(j\omega)$ is equal to $\mathbf{G}(e^{j\omega})$ when the strict band-limitedness assumption for the input signal (2) is fulfilled.

3. FREQUENCY MODEL OF THE BANDPASS SAMPLING AND BANDPASS FILTER BANK

The equation (2) corresponds to a strictly band limited, real valued input signal $x(t)$. It can be sub-sampled with a sampling frequency fulfilling the following constraints [10]:

$$\frac{2\Omega_2}{m+1} \leq \Omega_e \leq \frac{2\Omega_1}{m} \tag{20}$$

For the sake of simplicity, let us assume that $\Omega_2 - \Omega_1 = \pi$ and $m = 2l$, this allows to alias all the negative pulsations from the interval $(-\Omega_2, -\Omega_1)$ to the negative pulsations $(-\pi, 0)$ and all the positive pulsations form interval (Ω_1, Ω_2) to positive pulsations $(0, \pi)$. Then we have:

$$\Omega_e = 2\pi,\ \Omega_1 = l\Omega_e \text{ and } \Omega_2 = \left(l + \frac{1}{2}\right)\Omega_e. \tag{21}$$

This sampling frequency is valid only if there are no signal components at Ω_1 and Ω_2 [10].

To design the HFB ADC, we first need to calculate the equivalent-digital filter bank through

$$X(j\Omega)H_m(j\Omega) = V_m(j\Omega). \tag{22}$$

Next, after sampling, we obtain:

$$G_m(e^{j\omega}) = \sum_{n\in\mathbb{Z}} V_m\left(j(\omega - n\Omega_e)\right), \tag{23}$$

where $\omega \in (-\pi, \pi)$. Because of (21) the above sum has only two nonzero terms for $n = \pm l$ so

$$G_m(e^{j\omega}) = V_m(j(\omega - \Omega_1)) + V_m(j(\omega + \Omega_1)). \tag{24}$$

When (24) is calculated using regular Fourier Transform, the discrete frequencies used are:

$$\omega = \frac{2\pi k}{N}\ ,\ k = [-N/2, \dots, N/2 - 1]. \tag{25}$$

Therefore we obtain $G_m(e^{j\omega}) =$

$$\begin{cases} G_m\left(\frac{j2\pi k}{N} - \Omega_1\right) & k = [-N/2 + 1, \dots, -1], \\ G_m\left(\frac{j2\pi k}{N} + \Omega_1\right) & k = [1, \dots, N/2 - 1], \\ 0 & k = [-N/2,\ 0]. \end{cases} \tag{26}$$

Consequently the system of equations (19) is underdetermined and $\mathbf{G}_m(e^{j\omega})$ has no constraints for $\omega = -\pi$ and $\omega = 0$. As this situation arises from the fact that the input signal has no energy at these frequencies, the shape of $\mathbf{G}_m(e^{j\omega})$ could be set freely for $\omega = -\pi$ and $\omega = 0$. A straightforward solution that fulfills the hermitian symetry of the spectrum for real signals is to replace the null values of $G_m(e^{j0})$ and $G_m(e^{-j\pi})$ by the ones that are interpolated using for instance splines. In that case the bandpass filters at the edges of the band of the input signal (2) will become respectively a low pass and a high pass filters in base band after sampling.

Another approach is to sample the frequency line as follows :

$$\omega = \frac{2\pi(2k+1)}{2N}\ ,\ k = [-N/2, \dots, N/2 - 1]. \tag{27}$$

Thus instead of using regular Fourier transform we utilize this shifted one :

$$X(k) = \sum_{n=0}^{N-1} x(n)e^{-j\pi n(2k+1)/N}. \tag{28}$$

It is easy to check that functions $e^{-j\pi n(2k+1)/N}$ spans the frequency space like the traditional Fourier transform. The only difference is that the proposed transform is calculated at frequency points shifted by an half of a frequency bin.

$$e^{-j\pi n(2k+1)/N} = e^{-j\frac{2\pi nk}{N}} e^{-j\frac{1}{2}\frac{2\pi n}{N}}. \tag{29}$$

This discretization scheme involves implicitly an interpolation for the values at $G_m(e^{j0})$ and $G_m(e^{-j\pi})$ and in that case too, we get a low pass and a high pass filters in base band after sampling instead of the bandpass filters at the edges of the band of the input signal (2).

4. RESULTS OF THE HFB ADC SIMULATIONS IN FREQUENCY DOMAIN

The experimental distortion function of the HFB ADC system is defined as the ratio between input and output signals

$$T_x(e^{j\omega}) = \frac{\widehat{X}(e^{j\omega})}{X(j\omega)}, \tag{30}$$

where $X(j\omega)$ is the baseband equivalent spectrum of the continuous input signal perfectly bounded to the band B and down-converted to $\omega \in (-\pi, \pi)$. Combining (30) with (10), the following formula can be obtained

$$T_x(e^{j\omega}) = T_0(e^{j\omega}) + \underbrace{\sum_{l=1}^{M-1} T_l(e^{j\omega}) \frac{X(j\omega_M^{(l)})}{X(j\omega)}}_{\text{aliasing function}} \tag{31}$$

where, from (14), the theoretical distortion function is

$$T_0(e^{j\omega}) = \mathbf{G}^{(0)}(e^{j\omega})\mathbf{F}(e^{j\omega}). \tag{32}$$

The $\mathbf{G}^{(0)}(e^{j\omega})$ is the first row of the matrix $\mathbf{G}(e^{j\omega})$. Thus experimental aliasing of the system can be calculated as

$$T_a(e^{j\omega}) = T_x(e^{j\omega}) - T_0(e^{j\omega}). \tag{33}$$

In our tests the AFB was composed of eight sixth order bandpass Butterworth filters. The set-up of each test was composed of tree steps: system design, simulation and result checking. In this first step, the transfer functions $\mathbf{G}(e^{j\omega})$ are derived based on an assumed In-band to Out-band signal Power Radio (IOPR). Then the synthesis filter bank $\mathbf{F}(e^{j\omega})$ is obtained by solving equation (19). In the second step, the spectrum with a given IOPR (not necessarily the same as in the design step) of a test signal $X(j\Omega)$ is generated and processed by the HFB ADC. Finally the experimental distortion transfer and aliasing functions are calculated.

For the system design step, the bandwidth of the input signal was normalized to $1[\pi\text{rad}/s]$ and lies in the following interval $B = (-11, -10) \cup (10, 11)[\pi\text{rad/s}]$, while considering continuous frequency range was $\Omega \in (-20, 20)[\pi\text{rad}/s]$. The continuous input signal power was:

$$X(j\Omega) = \begin{cases} 1 & \Omega \in B \\ 10^{-\text{IOPR}/10} & \Omega \notin B \end{cases} \tag{34}$$

For the experimental results presented in this paper, the same input signal was used during design and simulation steps.

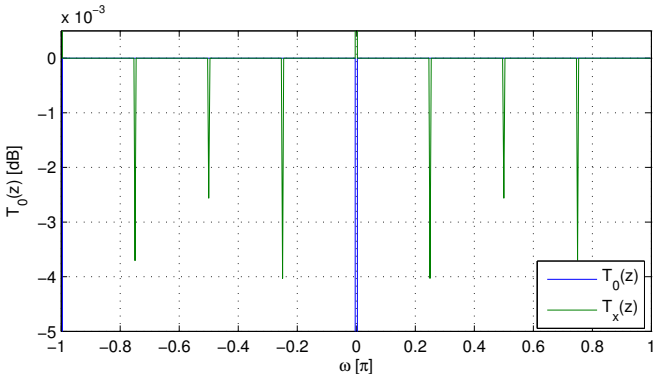

(a) Experimental Distortion functions

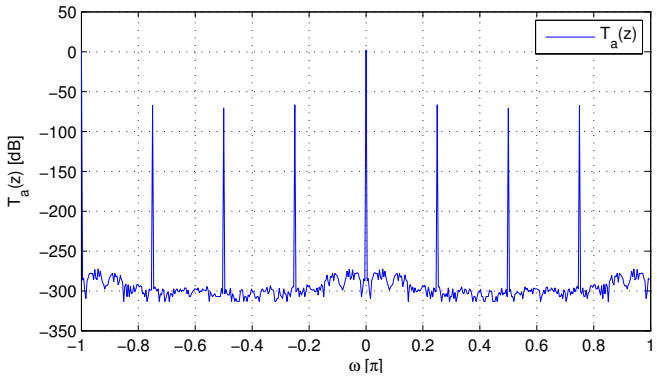

(b) Experimental Aliasing functions

Fig. 3. The effect of simulating HFB ADC using traditional Fourier transform, signal IOPR=20dB.

Figure 3 shows the distortion and aliasing transfer functions of the HFB ADC which was calculated using regular Fourier transform and spline interpolation. One can observe spikes which are appearing exactly at each multiple of Ω_e/M which is equal to $\pi/4$ in our test case. This occurs because of the sampling process which is modeled by the modulation matrix (9) followed by the up-samplers which mirrors the base band spectrum of each branch, especially the lower and the upper ones which are impacted by the lack of energy of the input signal at frequencies Ω_1 and Ω_2, which correspond to 0 and $-\pi$ in baseband, see (26).

Figure 4 presents the distortion and aliasing transfer functions of the system calculated using shifted frequency transform. It is clear that the proposed transform allows to suppress spectrum spikes and improve the convergence towards

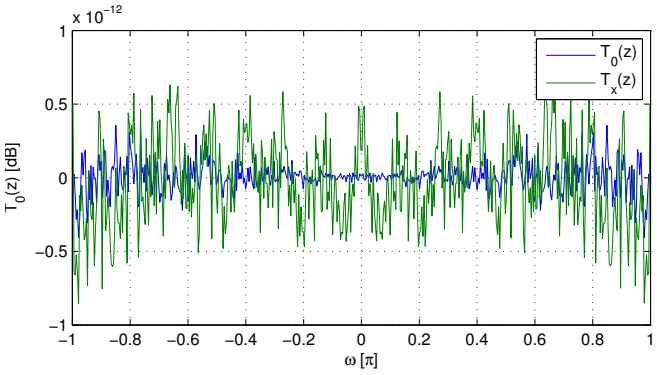

(a) Experimental distortion functions

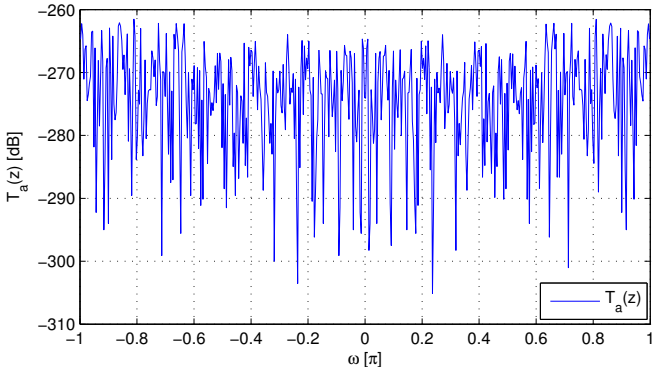

(b) Experimental aliasing functions

Fig. 4. Simulation result using proposed frequency transform, signal IOPR=20dB.

PR condition for all frequencies.

5. CONCLUSION

This paper addresses the modelization of a bandpass HFB ADC architecture designed to sample wide-band signals directly at RF or IF frequency. The design and simulation methodology of the bandpass HFB ADC system in frequency domain was presented. An equivalent-digital analysis filter bank (19) was proposed to model the bandpass sampling of a wide-band signal directly in RF band.

Two different schemes were proposed to model the pass-band to baseband aliasing in frequencies due to sampling. This two different schemes exhibit different level of quality regarding the PR property. Simulation results show that it is possible to reach PR condition for the desired IOPR.By using the shifted Fourier transform we are able to suppress the spikes observed in distortion and aliasing transfer functions.

All simulations were performed utilizing floating point arithmetics while one would expect the use of fixed point numbers. Indeed, signals at the output of the ADCs should be represented using a fixed number of bits modeling the chosen ADC. However using fixed point numbers during simulation causes several additional problems, which are beyond the scope of this paper and will be addressed in future work.

6. REFERENCES

[1] P. Vaidyanathan, "Multirate digital filters, filter banks, polyphase networks, and applications: a tutorial," *Proceedings of the IEEE*, vol. 78, no. 1, pp. 56–93, Jan. 1990.

[2] J. Brown, "Multi-channel sampling of low-pass signals," *Circuits and Systems, IEEE Transactions on*, vol. 28, no. 2, pp. 101–106, Feb. 1981.

[3] C. Vogel and H. Johansson, "Time-interleaved analog-to-digital converters: status and future directions," in *Circuits and Systems, 2006. ISCAS 2006. Proceedings. 2006 IEEE International Symposium on*, 2006.

[4] P. Löwenborg, H. Johansson, and L. Wanhammar, "A survey of filter bank A/D converters," in *Swedish System-on-chip Conference*, 2001.

[5] A. Lesellier, O. Jamin, J. Bercher, and O. Venard, "Design, optimization and calibration of an HFB-based ADC," in *New Circuits and Systems Conference (NEWCAS), 2011 IEEE 9th International*, Jun. 2011, pp. 317–320.

[6] C. Lelandais-Perrault, T. Petrescu, D. Poulton, P. Duhamel, and J. Oksman, "Wideband, bandpass, and versatile hybrid filter bank A/D conversion for software radio," *IEEE Transactions on Circuits and Systems I: Regular Papers*, vol. 56, no. 8, pp. 1772–1782, Aug 2009.

[7] J. Elbornsson, F. Gustafsson, and J.-E. Eklund, "Blind equalization of time errors in a time-interleaved ADC system," *Signal Processing, IEEE Transactions on*, vol. 53, no. 4, pp. 1413–1424, April 2005.

[8] B. Murmann, "A/D converter trends: Power dissipation, scaling and digitally assisted architectures," in *Custom Integrated Circuits Conference, 2008. CICC 2008. IEEE*, Sep 2008, pp. 105–112.

[9] A. Lesellier, O. Jamin, J. Bercher, and O. Venard, "Design, optimization and realization of an HFB-based ADC," in *Circuit Theory and Design (ECCTD), 2011 20th European Conference on*, Aug. 2011, pp. 138–141.

[10] R. Vaughan, N. Scott, and D. White, "The theory of bandpass sampling," *IEEE Transactions on Signal Processing*, vol. 39, no. 9, pp. 1973–1984, Sep. 1991.